In Vitro Th17-Polarized Human CD4+ T Cells Exacerbate Xenogeneic Graft-versus-Host Disease

Loïc Delens[1], Grégory Ehx[1], Joan Somja[2], Louise Vrancken[1,3], Ludovic Belle[1], Laurence Seidel[4],
Céline Grégoire[1,3], Gilles Fransolet[1], Caroline Ritacco[1], Muriel Hannon[1], Sophie Dubois[1],
Yves Beguin[1,3], Frédéric Baron[1,3], Sophie Servais[1,3,*]

[1] Hematology Research Unit, Interdisciplinary Group of Applied Genoproteomics, University of Liège, Liège, Belgium

[2] Department of Pathology, Liège University Hospital Center, Liège, Belgium

[3] Division of Hematology, Department of Medicine, Liège University Hospital Center, Liège, Belgium

[4] Department of Biotatistics, Service des Informations Médico-Economiques (SIMÉ), Liège University Hospital Center, Liège, Belgium

A B S T R A C T

Acute graft-versus-host disease (aGVHD) is a severe complication of allogeneic hematopoietic stem cell transplantation. The role of Th17 cells in its pathophysiology remains a matter of debate. In this study, we assessed whether enrichment of human peripheral blood mononuclear cells (PBMCs) with in vitro Th17-polarized CD4+ T cells would exacerbate xenogeneic GVHD (xGVHD) into NOD-scid IL-2Rγ null (NSG) mice. Naive human CD4+ T cells were stimulated under Th17-skewing conditions for 8 to 10 days and then coinjected in NSG mice with fresh PBMCs from the same donor. We observed that Th17-polarized cells engrafted and migrated toward xGVHD target organs. They also acquired a double-expressing IL-17A+IFNγ+ profile in vivo. Importantly, cotransfer of Th17-polarized cells (1×10^6) with PBMCs (1×10^6) exacerbated xGVHD compared with transplantation of PBMCs alone (2×10^6). Furthermore, PBMC cotransfer with Th17-polarized cells was more potent for xGVHD induction than cotransfer with naive CD4+ T cells stimulated in nonpolarizing conditions (Th0 cells, $1 \times 10^6 + 1 \times 10^6$ PBMCs) or with Th1-polarized cells ($1 \times 10^6 + 1 \times 10^6$ PBMCs). In summary, our results suggest that human Th17-polarized cells can cooperate with PBMCs and be pathogenic in the NSG xGVHD model.

© 2018 American Society for Blood and Marrow Transplantation.

INTRODUCTION

Acute graft-versus-host disease (aGVHD) remains a major cause of transplantation-related mortality after allogeneic hematopoietic stem cell transplantation (alloHSCT). The immunobiology of aGVHD is complex and involves an intricate network of immune cells [1-3]. Among these cells, donor T cells are considered the main drivers and effectors of aGVHD reactions, as demonstrated by the low incidence of aGVHD observed in patients who undergo T cell-depleted alloHSCT [4]. During aGVHD, donor T cells react against host foreign antigen/HLA complexes through both direct and indirect allorecognition via their T cell receptors, and proliferate through engagement of costimulatory molecules. The third signal is provided by cytokines that further promote T cell polarization.

Whereas interleukin (IL)-12 or IL-4 stimulation induces differentiation toward interferon (IFN)-γ-producing T helper (Th)1 cells or IL-4-producing Th2 cells, respectively, transforming growth factor (TGF)-β, IL-6, IL-1β, IL-21, and IL-23 drive the development of IL-17-producing Th17 cells [5]. Th17 cells are now widely considered key mediators in several inflammatory diseases, such as experimental autoimmune encephalomyelitis and colitis. Whether these cells are also involved in the pathophysiology of alloimmune inflammation in aGVHD has remained an open question. In fact, although a growing amount of data support a role of Th17 cells in aGVHD in preclinical mouse models [6-11], studies in humans have reported conflicting results, suggesting [12-15] or dismissing [16-18] their involvement.

Significant differences exist between human and murine immune systems, and a major limitation of animal models remains their limited predictive value in human diseases [19]. An example can be drawn from the recent experience with IL-17 blockade in inflammatory bowel disorders, in which several studies in mice had linked IL-17 to the pathogenesis of colitis, but treatment with anti-IL-17A and anti-IL-17RA antibodies was found to ultimately exacerbate the disease in humans [20-22]. To bridge these limitations, humanized mouse models may serve as an attractive intermediate platform between animal models and projection to the clinic by offering the opportunity to study the behavior of human immune cells in vivo.

Over the past several decades, humanized murine models of xenogeneic GVHD (xGVHD) have been developed via the injection of human peripheral blood mononuclear cells (PBMCs) into severely immunodeficient NOD/Shi-scid IL2rγ-null (NOG) or NOD/LtSz-scid IL2rγ-null (NSG) mice [23-32]. These models are T cell dependent, and main triggers of T cell activation and expansion are xenogeneic MHC (H-2) class I and class II molecules [23,30,33,34] and xenogeneic costimulatory signals [27,35]. Previous studies have demonstrated a crucial interplay between CD4$^+$ and CD8$^+$ T cells during xGVHD [23,35]; however, the concrete role of individual T cell subsets has not yet been fully elucidated.

More specifically, little is known about the potential implication of Th17 cells in xGVHD pathogenesis in NOG/NSG mice. Indeed, although some groups have reported the presence of human Th17 cells at the time of xGVHD, Th17 cells represent only a small fraction of CD4$^+$ T cells in blood, lymphoid tissue, and xGVHD target organs [23,26,34,36]. This may be due to low levels of human pro-Th17 cytokines in that model, which limit naive cell polarization toward Th17 fate in vivo after their transfer in mice. For example, low serum levels of human IL-6 were measured in xGVHD mice [37,38], and murine IL-6 does not bind to the human IL-6 receptor [39,40]. However, indirect observations, have suggested that Th17 cells, albeit infrequent in numbers, could participate in xGVHD pathogenesis [36,41]. Among these observations, IL-21 blockade was found to decrease IL-17-producing cells in target organs and to significantly reduce xGVHD [36]. Nevertheless, it is difficult to conceive a Th17-dependent pathway as the exclusive mechanism for xGVHD prevention by IL-21 blockade, considering that this strategy also increases regulatory T cell (Treg) numbers and decreases the proportions of IFNγ- and granzyme B-secreting T cells. More recently, Ito et al [23] reported that after transplantation of purified CD4$^+$ human T cells into NOG mice, Th17 cells accumulated in the skin and induced IL-17-mediated skin inflammation and lesions.

In the present study, we explored the potency of in vitro Th17-polarized human CD4$^+$ T cells to participate in xGVHD in NSG mice. Because Th17 cells do not mediate their immune effects independently but rather work in concert with other cells, we evaluated whether the administration of Th17-polarized cells could cooperate with whole PBMCs in the induction of xGVHD.

MATERIALS AND METHODS
In Vitro Polarization of Human Naive CD4$^+$ T Cells
Human whole peripheral blood (PB) was obtained from healthy adult volunteers (age 20 to 35 years) following written informed consent. PBMCs were isolated by Ficoll-Paque density centrifugation (GE Healthcare, Freiburg, Germany). Naive CD4$^+$CD45RA$^+$CD62L$^+$CD25$^-$ cells were sorted by high-speed flow cytometry (FACSAria III; BD Biosciences, San Jose, CA) to >98% purity as verified by postsorting analysis. Sorted cells were plated in 96-well round-bottomed plates at a density of 1×10^5 cells per well in XVIVO 15 media (Lonza, Basel, Switzerland), along with anti-CD3/anti-CD28- coated beads (1:1 bead cell ratio; Invitrogen, Carlsbad, CA). Depending on the type of experiment, cells were cultured in nonpolarizing conditions (no cytokines), Th17-polarizing conditions (25 ng/mL rhuIL-6, 6.25 ng/mL rhuTGF-β1, 12.5 ng/mL rhuIL-1β, 25 ng/mL rhuIL-21, and 25 ng/mL rhuIL-23 [all from PeproTech, Rocky Hill, NJ], 500 ng/mL anti-human IFNγ antibody [NIB42; BioLegend, San Diego, CA], 500 ng/mL anti-human IL-2 antibody [5334; R&D Systems, Minneapolis, MN], and 40 mM NaCl), as described previously [42], or Th1-polarizing conditions (20 ng/mL rhuIL-12p70, 5 ng/ml rhuIL-2 [both from PeproTech] and 500 ng/ml anti-human IL-4 antibody [8D4-8; BioLegend]). Medium was changed every 3 to 4 days, and cells were harvested after a total of 8 to 10 days of culture. Cell suspensions obtained at harvest were designated as nonpolarized Th0 cells, Th17-polarized cells, and Th1-polarized cells.

Induction of xGVHD in NSG Mice
Immunodeficient NSG mice were used for all experiments (see **Supplementary Materials and Methods**). For xGVHD induction, 8- to 12-week-old NSG mice were irradiated (2.5 Gy total body irradiation, [137Cs source gamma cell irradiator 40; Nordion, Ottawa, Canada]) on day -1 and underwent transplantation (lateral tail vein injection) on day 0 with either PBMCs alone or PBMCs combined with in vitro cultured CD4$^+$ T cells (Th17-polarized, Th1-polarized, or nonpolarized Th0 cells) from the same donor. Mice were monitored daily for general well-being and weighed 3 times weekly. The severity of xGVHD was also recorded thrice weekly using a scoring system that incorporates 4 clinical parameters—weight loss, hunching, lethargy, and anemia—each scored from 0 (absent) to 2 (severely marked), as described previously [25,26]. An xGVHD score ≥6/8 or weight loss ≥20% were considered ethical limit points, as requested by our Institutional Ethics Committee. Mice were euthanized when reaching the ethical limit point or earlier if sacrifice was planned at a predefined time point. Depending on the experiment, serial PB samples were collected at days +14 and +21 after human cell transplantation. Furthermore, at the time of necropsy, PB, spleen, bone marrow (BM), liver, and lungs were harvested as well. Methods used for mononuclear cell isolation from peripheral organs are described in **Supplementary Materials and Methods**. Within each individual experiment, all groups of mice underwent transplantation with cells from the same donor. To limit interdonor variability, most of the experiments were replicated with at least 2 different donors. All experimental protocols and procedures were approved by the Institutional Animal Care and Use Ethics Committee of the University of Liège (certification 1544).

Graft-versus-Tumor Effects
To investigate graft-versus-tumor (GVT) effects, we used THP-1 cells (a human tumoral cell line derived from an acute monocytic leukemia patient, TIB-202; American Type Culture Collection, Manassas, VA) transfected with a lentiviral vector containing reporter genes coding firefly luciferase (THP-1-luc), as described previously [26]. Eight- to 12-week-old NSG mice were irradiated on day -1 and underwent transplantation on day 0 with either PBMCs alone or with PBMCs combined with in vitro cultured CD4$^+$ T cells (Th17-polarized, Th1-polarized, or nonpolarized Th0 cells) from the same donor (see above for the xGVHD model). At 14 days after transplantation, mice also received an s.c. injection (in the left flank) of 1×10^6 THP-1-luc cells suspended in 200 μL of a 50/50 PBS (Lonza) and Matrigel (Corning, Tewksbury, MA) solution. This enables THP-1-luc cells to proliferate locally and to form subcutaneous tumors at the site of injection. Tumor growth was evaluated by measuring bioluminescence at day +21 after THP-1-luc injection (see **Supplementary Materials and Methods**). At day +49 after THP-1-luc injection, mice were sacrificed, and tumors were dissected and weighted. As a positive control, another group of mice also received s.c. injections of THP-1-luc cells without receiving either irradiation or transplantation with human immune cells (THP-1 control group).

Flow Cytometry Analyses
Mononuclear cells were stained with various combinations of fluorescence-conjugated anti-human antibodies (**Supplementary Materials and Methods**). For extracellular staining, cells were incubated with appropriate antibodies for 20 minutes at 4°C and then washed twice with PBS and 3% FBS. For FOXP3 and cytokine intracellular staining, cells were fixed and permeabilized with the FOXP3 Staining Buffer Set (Thermo Fisher Scientific , Waltham, MA), according to the manufacturer's instructions. For intracellular cytokine staining, cells were stimulated for 4h with Cell Stimulation Cocktail Plus Protein Transport Inhibitors (Invitrogen) in XVIVO 15 media (Lonza), followed by fixation, permeabilization, and staining with appropriate antibodies according to the manufacturer's instructions. Data were acquired using a FACSCanto II flow cytometer (BD Biosciences) and analyzed with FlowJo 7.0 (TreeStar, Ashland, OR). For absolute count calculation, absolute white blood cells were counted with a Sysmex XS-800i hematology analyzer (Sysmex, Norderstedt, Germany) before antibody staining.

Other Analyses
The RT-qPCR assay, carboxyfluorescein diacetate succinimidyl ester (CFSE) dilution assay, quantification of serum cytokine levels, histology, and immunohistochemistry are described in Supplementary Materials and Methods.

Statistical Analyses
Data are presented as individual observations with median, unless specified otherwise. Comparisons between groups were made with 1-way analysis of variance (ANOVA) with the Scheffe post hoc procedure. To normalize their distribution, some variables underwent prior logarithmic or square root transformation. Survival curves were plotted using Kaplan-Meier estimates, and comparisons between groups were done using the log-rank test. Weight loss over time was analyzed using a generalized linear mixed model, and the evolution of xGVHD score over time was analyzed using a repeated ordinal logistic model. Weight and xGVHD score at death were carried forward after death. Multivariate Cox models adjusted for PBMC donor and mouse sex and weight were also performed for most of the analyses. Results were

considered significant at the 5% level ($P < .05$). Statistical analyses were carried out with SAS version 9.4 (SAS Institute, Cary, NC), and figures were prepared with Prism 5.0 (GraphPad Software, La Jolla, CA).

RESULTS

In Vitro Th17-Polarized Cells

We examined the secreting profile of human naive CD4$^+$ T cells after 8 to 10 days of in vitro stimulation under the Th17-polarizing condition and under the nonpolarizing (Th0) condition (Figure 1). Whereas Th0 condition naturally resulted in an IFNγ^+IL-17A$^-$ (Th1)-expressing profile in a substantial proportion of cells, cell suspensions obtained from Th17-polarizing cultures were characterized by a median of 10% (range, 7% to 38%) of IL-17A-expressing cells and a low proportion of IFNγ^+IL-17A$^-$ cells (median 2%; range, 1% to 8%) (Figure 1**A and B**). Most IL-17A$^+$CD4$^+$ cells did not coexpress IFNγ. Cells from Th17-polarizing cultures also displayed higher relative expression of IL17A, RORC (Th17-specific master transcription factor), and IL23R mRNA compared with Th0 cells, along with minimal expression of TBX21 (TBET) mRNA (Figure 1**C**). In both conditions, the expression of IL-4 (a cytokine of Th2 lineage) was minimal (<2%) (data not shown). Taken together, these results show that Th17-polarized cells could be generated from human naive CD4$^+$ T cells in vitro. However, in contrast to previous reports with murine cells [7,43-45], a significant fraction of human CD4$^+$ cells remained IL-17A$^-$IFNγ^-IL-4$^-$ unpolarized after 8 to 10 days of culture.

No good correlation was obtained between IL-17A intracellular staining and surface expression of CCR6 and CD161, 2 usual markers of Th17 cells [46] (data not shown). Because this precluded the possibility to perform CCR6$^+$CD161$^+$ FACS sorting of Th17 cells, we decided to use total cell suspension for mouse injections. To ensure the transfer of at least 100,000 IL-17A$^+$ cells per recipient mouse, we elected to use only Th17-polarized cell suspensions with a minimal yield of 10% of IL-17A$^+$CD4$^+$ cells. Specifically, this was achieved in 60% of cultures, and the Th17-polarized cell suspensions used in mouse experiments described below had a median of 21.5% (range, 10% to 38%) IL-17A$^+$ CD4$^+$ T cells.

We also checked that in vitro generated cells were not exhausted and were able to undergo additional rounds of division in vivo after transfer in NSG mice. Th17-polarized and nonpolarized Th0 cells, as well as CD4$^+$ T cells derived from freshly isolated PBMCs (control), were loaded with CFSE and then transplanted into irradiated NSG mice (4×10^6 cells/mouse). Mice were sacrificed at day +3. Human CD4$^+$ T cells and CFSE signals were detected in PB as well as in spleen and peripheral organs at this early time point. Interestingly, cultured cells (and more specifically, Th17-polarized cells), demonstrated high proliferative activity in vivo after transfer (**Supplementary Figure S1**).

Impact of PBMC Cotransplantation with Th17-Polarized Cells on xGVHD

In a first set of experiments, we investigated xGVHD in NSG mice cotransplanted with PBMCs (1×10^6 per mouse) and Th17-polarized cells (1×10^6 per mouse, Th17 coinjected group) and in mice transplanted with 2×10^6 PBMCs (PBMC group). To prevent interdonor variability, the experiment was replicated 4 times with 4 different donors. As shown in Figure 2**A**, Th17 coinjection led to significantly shorter survival (median survival, 29 days for Th17 coinjected mice versus 53 days for PBMC mice; $P = .015$). The higher lethality was confirmed in a multivariate Cox regression model adjusted for PBMC donor and mouse sex and weight (hazard ratio [HR], 2.9; 95% CI, 1.4 to 5.9; $P = .004$). Similarly, the clinical severity of xGVHD and the rate of weight loss were also aggravated in Th17 coinjected mice (Figure 2**B and C**). Of note, we also observed a significant impact of the
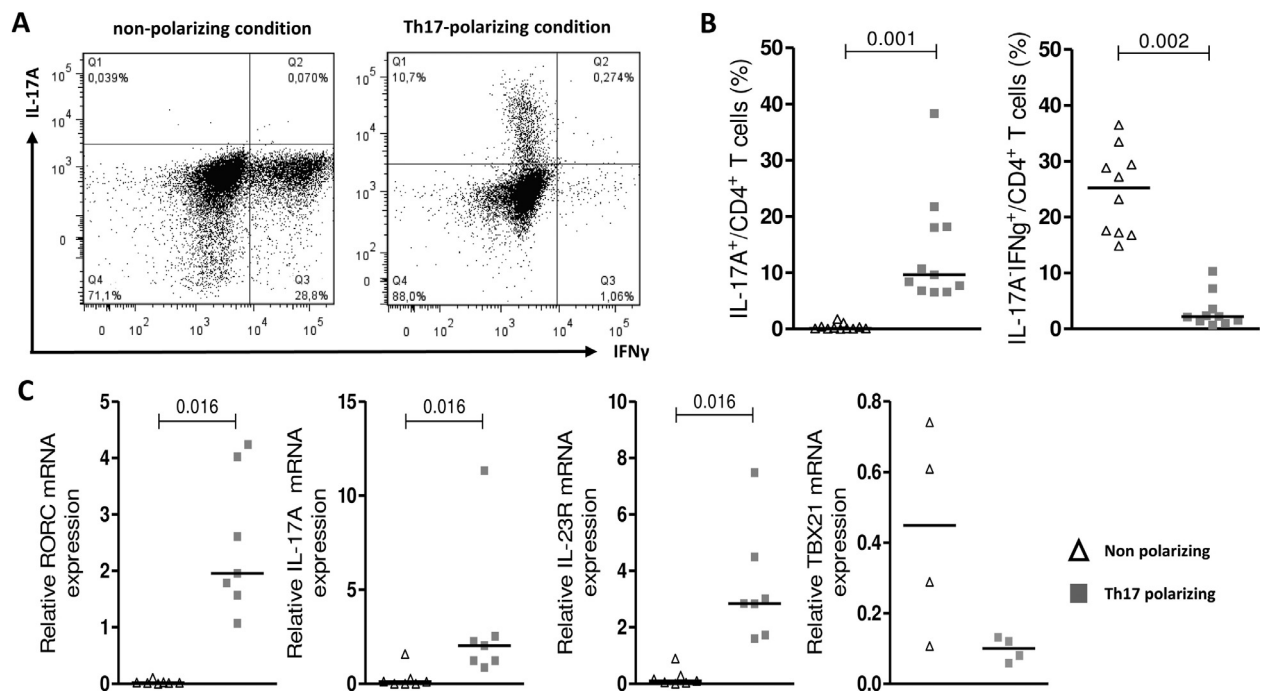
Figure 1. Human naive T cells cultured under Th17-polarizing and nonpolarizing conditions. Human naive CD4$^+$ T cells were stimulated with anti-CD3/anti-CD28 coated beads in either Th0-nonpolarizing (no cytokine) or Th17-polarizing (Th17-skewing cytokines and hypernatremia) conditions. After 8 to 10 days of culture, cells were harvested for flow cytometry and/or RT-qPCR analyses. (A) Representative FACS plot of IL-17A versus IFNγ. (B) frequencies of IL-17A$^+$ and IL17A$^-$ IFNγ^+ cells among CD4$^+$ cells (flow cytometry). (C) relative mRNA expression of RORC, IL-17A, IL-23R, and TBX21 (TBET) normalized to TBP (RT-qPCR). White triangles denote cells cultured in the Th0-nonpolarizing condition, and gray squares denote cells cultured in the Th17-polarized condition. The Wilcoxon rank-sum test was used for comparisons between the 2 conditions.
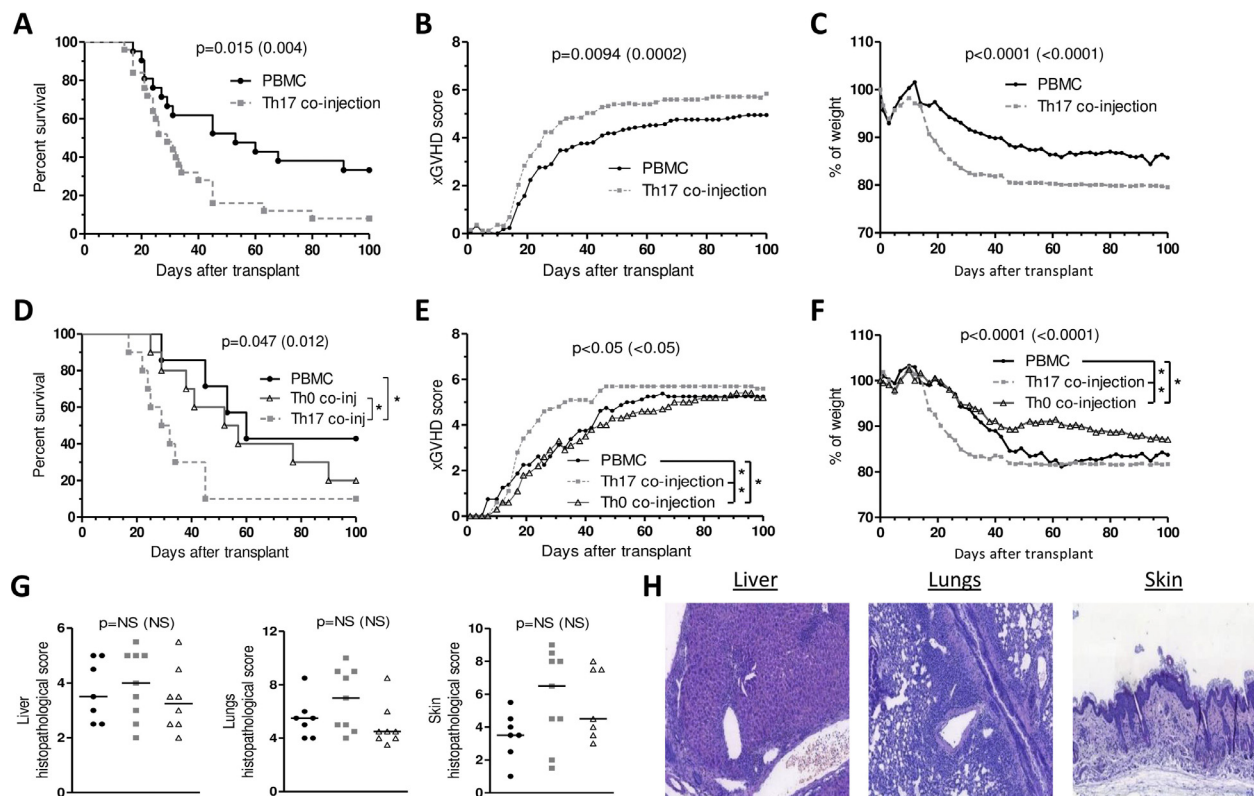
Figure 2. Impact of PBMC cotransplantation with Th17-polarized cells on xGVHD. NSG mice were irradiated (2.5 Gy total body irradiation) and underwent transplantation with 2×10^6 PBMCs alone (PBMC mice), with 1×10^6 PBMCs combined with 1×10^6 Th17-polarized cells (Th17 coinjected mice), or with 1×10^6 nonpolarized Th0 cells (Th0 coinjected mice) from the same donor. (A to C) Comparisons of survival (A), xGVHD score (B), and weight loss (C) between PBMC mice (n = 21) and Th17 coinjected mice (n = 25). Combined data from 4 replicate experiments with 4 different donors are shown. (D to F) Comparisons of survival (D), xGVHD score (E), and weight loss (F) in PBMC mice (n = 7), Th17 coinjected mice (n = 10), and Th0 coinjected mice (n = 10). Combined data from 2 replicate experiments with 2 different donors are shown. (G) xGVHD histopathological scores in liver, lungs, and skin tissue specimens at day +21 after transplantation. (H) Representative pictures (magnification 10×) of hematoxylin and eosin (H&E) staining of liver, lung, and skin tissues at day +21 in Th17 coinjected mice. Data are from a single experiment with 1 donor, 7 PBMC mice, 8 Th0 coinjected mice, and 9 Th17 coinjected mice. For xGVHD score and weight loss, data are shown as means. *P* values in parentheses refer to a multivariate Cox model adjusted for PBMC donor, mouse sex, and weight. For comparisons among PBMC, Th17 coinjected, and Th0 coinjected mice (D-F), global *P* values (1-way ANOVA) are shown, along with 2-by-2 group comparisons with the Scheffe post hoc procedure (*P < .05). Black circles denote PBMC mice; gray squares, Th17 coinjected mice; white triangles, Th0 coinjected mice.

PBMC donor on survival (*P* = .016) and xGVHD score (*P* < .05) in the multivariate analyses.

We further performed another set of experiments with an additional comparative group of mice cotransplanted with PBMCs and nonpolarized Th0 cells ($1 \times 10^6 + 1 \times 10^6$ per mouse, Th0 coinjected group). We observed significant differences in survival between groups (univariate analysis, *P* = .047; multivariate analysis, *P* = .012) with increased risk of lethality for Th17 coinjected mice compared with PBMC mice (HR, 7.1; 95% CI, 1.9 to 26.3, multivariate analysis) and Th0 coinjected mice (HR, 3.1; 95% CI, 1.1 to 9.1, multivariate analysis). In contrast, survival was similar in Th0 coinjected and PBMC mice (Figure 2D). XGVHD score and weight loss analyses also indicated aggravated xGVHD among Th17 coinjected mice compared with the other 2 groups (Figure 2E and F).

In another set of experiments, we sacrificed mice at day +21 after transplantation to assess xGVHD pathology in target tissues (liver, lungs, and skin) (hematoxylin and eosin [H&E] stain; Figure 2G and H). In each of these organs, we noted lymphoid infiltrates, tissue lesions (including endotheliitis and alveolar and bronchial alterations in the lungs; portal tract expansion, endotheliitis, and parenchymal alteration in the liver; and epidermal hyperplasia and epidermal and follicular dyskeratosis in the skin), and typical signs of xGVHD, such as apoptotic bodies and bile plugs. When integrating these observations into a xGVHD histopathological scoring system (**Supplementary Materials and**

Methods), we noted trends for higher scores in lungs and skin for Th17 coinjected mice compared with the other 2 groups, although the differences did not reach statistical significance (Figure 2**G**).

Regarding the clinical phenotype of xGVHD, no difference was observed between groups except for extensive areas of fur loss that developed in some Th17 coinjected mice (Figure 3**A**). These cutaneous manifestations occurred after a delay of 40 to 70 days after human cell transplantation and concerned 4 of the 7 Th17 coinjected mice that survived beyond day +40. In 2 of these mice, skin specimens were harvested by the time of necropsy for histopathological analyses, which revealed severe skin xGVHD histopathological scores (10.5 and 16.5) with epidermal hyperplasia, marked epidermal and follicular dyskeratosis, basal cell layer vacuolization, and dermal fibrosis (Figure 3**B**).

Characterization of Circulating Human T Cells in Mice Cotransplanted with PBMCs and Th17-Polarized Cells

We analyzed human T cells in PB of PBMC mice, Th17 coinjected mice, and Th0 coinjected mice at day +14 post-transplantation. Human CD45+ chimerism was similar in all groups (Figure 4**A**). In comparison with PBMC mice, we noted higher CD4+/CD8+ T cell ratio and higher absolute numbers of CD4+ T cells in PB of Th17 and Th0 coinjected animals (Figure 4**B and D**). In Th17-coinjected mice, circulating CD4+ T cells were characterized by a significantly higher proportion of IL-17A+ cells (median, 13.2%) compared with PBMC and Th0 coinjected mice
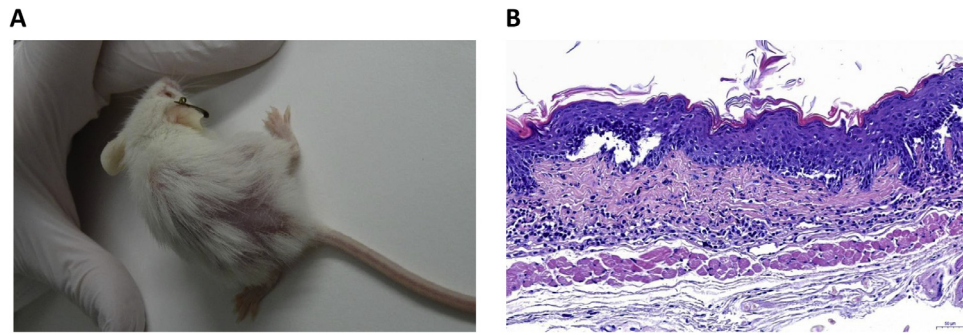
Figure 3. Late cutaneous manifestations in surviving Th17 coinjected mice. (A) Representative picture of a Th17-coinjected mouse (10^6 PBMCs + 10^6 Th17-polarized cells) at day +40 after transplantation. (B) H&E staining of skin tissues (magnification $20\times$) from a Th17-coinjected mouse (10^6 PBMCs + 10^6 Th17-polarized cells) with a cutaneous phenotype, sacrificed at day +45 after transplantation.
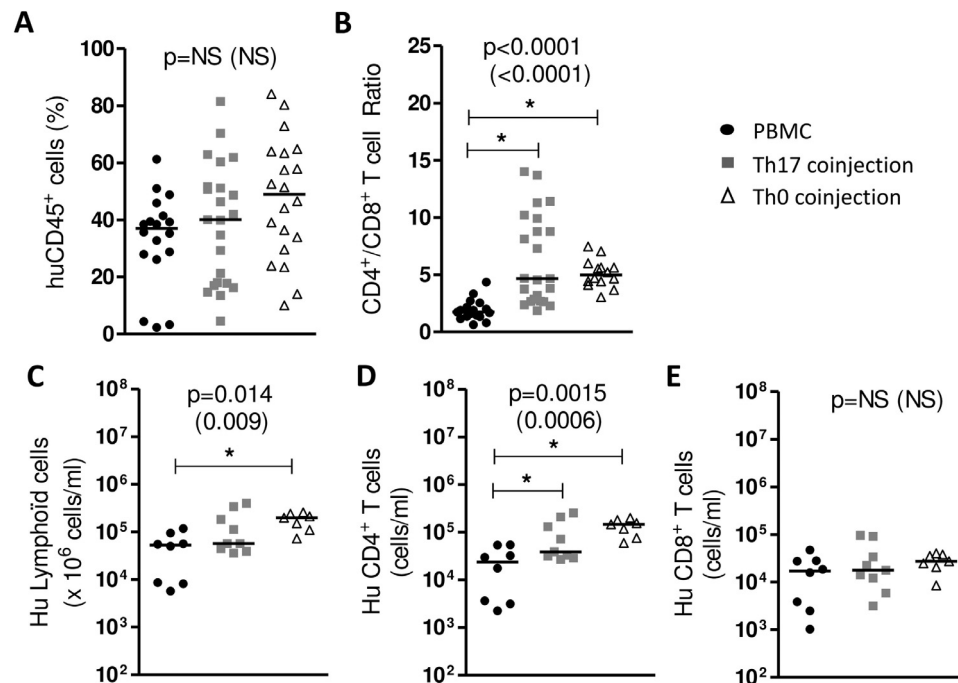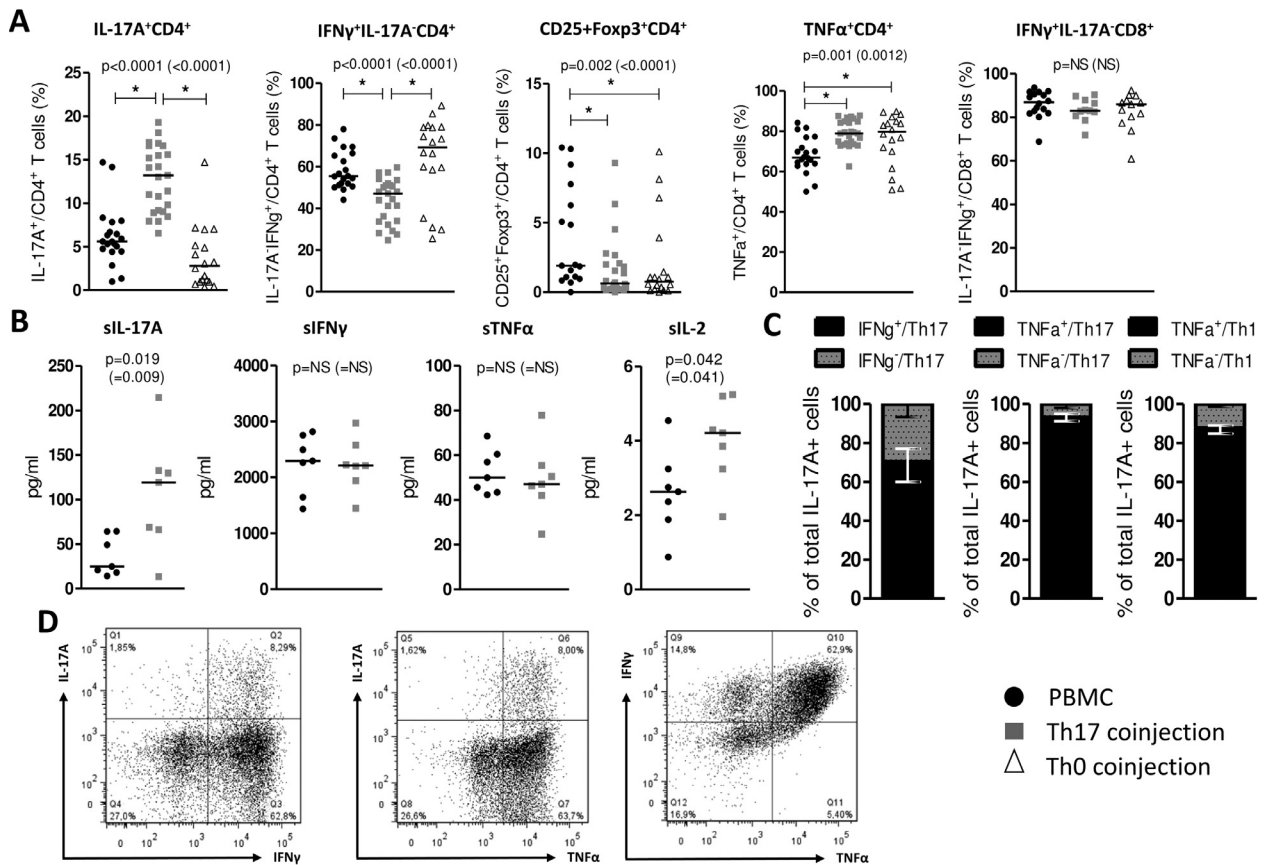

Figure 4. Circulating human T cells in PB of PBMC, Th17 coinjected and Th0 coinjected mice at day +14 after transplantation. NSG mice were irradiated (2.5 Gy total body irradiation) and then underwent transplantation with 2×10^6 PBMCs alone (PBMC mice), with 1×10^6 PBMCs combined with 1×10^6 Th17-polarized cells (Th17 coinjected mice), or with 1×10^6 nonpolarized Th0 cells (Th0 coinjected mice) from the same donor. Peripheral blood samples were collected at day +14 after transplantation for flow cytometry analyses. (A and B) Human lymphoid chimerism (A) and CD4$^+$/CD8$^+$ human T cell ratio (B); combined data from 3 replicate experiments with 3 different donors. (C to E) Absolute counts of human CD45$^+$ lymphoid cells (C), CD4$^+$ T cells (D), and CD8$^+$ T cells (E); analyses from 1 experiment with a single donor. Global *P* values (1-way ANOVA) are shown, along with 2-by-2 group comparisons with the Scheffe post hoc procedure (*$P < .05$). *P* values in parentheses refer to a multivariate Cox model adjusted for PBMC donor, mouse sex, and weight. Prior logarithmic transformation was applied for CD4/CD8 T cell ratio, and prior square root transformation was applied for absolute numbers of cells. Black circles denote PBMC mice; gray squares, Th17 coinjected mice; white triangles, Th0 coinjected mice.

(median, 5.6% and 2.8%, respectively) (Figure 5A). Accordingly, higher absolute numbers of IL-17A$^+$CD4$^+$ T cells (**Supplementary Figure S2**) and higher serum titers of IL-17A were also measured in Th17 coinjected mice (Figure 5B). Interestingly, although very few in vitro generated IL-17A$^+$ cells expressed IFNγ (see above), the majority of circulating IL-17A$^+$CD4$^+$ T cells acquired a double IL-17A$^+$IFNγ^+ secreting profile in vivo (Figure 5C and D).

PB from Th17 coinjected mice also revealed a significantly lower proportion of IL-17A$^-$IFNγ^+ (Th1) CD4$^+$ T cells compared to PBMC and Th0 coinjected animals (Figure 5A). Regarding CD4$^+$CD25$^+$FOXP3$^+$ Treg and TNFα-expressing CD4$^+$ T cells, PB composition in Th17 coinjected mice was similar to that observed in Th0 coinjected mice, namely with a lower

proportion of Tregs and a higher proportion of TNFα^+CD4$^+$ T cells compared with PBMC recipients (Figure 5A). TNFα was expressed by most of IL-17A$^+$ (Th17) and IL-17A$^-$IFNγ^+ (Th1) CD4+ T cells (Figure 5C and D). Finally, no differences in CD8$^+$ T cell subsets were observed among the groups. Most CD8$^+$ T cells were IL-17A$^-$IFNγ^+ CD8$^+$ T cells (Tc1) (Figure 5A), whereas only a very low (<1%) proportion of IL-17A$^+$CD8$^+$ T cells (Tc17) were detected in all groups (data not shown).

Similar trends were observed when comparing absolute counts of T cell subsets, with the exception of the number of IL-17A$^-$IFNγ^+ (Th1) cells, which was similar in Th17 coinjected and PBMC mice, because of higher numbers of circulating total CD4$^+$ T cells in Th17 coinjected mice (**Supplementary Figure S2**). However, their numbers remained lower than

Figure 5. Circulating human CD4$^+$ T cell subsets and cytokines in PB of PBMC, Th17 coinjected, and Th0 coinjected mice at day +14 after transplantation. NSG mice were irradiated (2.5 Gy total body irradiation) and then underwent transplantation with 2×10^6 PBMCs alone (PBMC mice), with 1×10^6 PBMCs combined with 1×10^6 Th17-polarized cells (Th17 coinjected mice), or with 1×10^6 nonpolarized Th0 cells (Th0 coinjected mice) from the same donor. Peripheral blood samples were collected at day +14 after transplantation for luminex and flow cytometry analyses. (A to C) Frequencies of CD4$^+$ and CD8$^+$ T cell subsets (A), cytokine serum concentrations (B), and frequencies of IFNγ- and TNFα-expressing cells (C) for Th17 coinjected mice. Data are median with interquartile range. Data were combined from 3 replicate experiments (A and C) or were from a single experiment (B) (analysis not performed for Th0 coinjected mice). (D) Representative FACS plots from a Th17 coinjected mouse. Global *P* values (1-way ANOVA) are shown, along with 2-by-2 group comparisons with the Scheffe post hoc procedure (*$P < .05$). *P* values in parentheses refer to a multivariate Cox model adjusted for PBMC donor and mouse sex and weight. Prior logarithmic transformation was applied for percentage of Tregs. Black circles denote PBMC mice; gray squares, Th17 coinjected mice; white triangles, Th0 coinjected mice.

those seen in Th0 coinjected mice. We further measured serum titers of IFNγ and TNFα and found no differences between Th17 coinjected and PBMC mice (Figure 5**B**). Low IL-2 titers were detected, which were higher in the Th17 coinjected mice (Figure 5**B**).

PB samples were also collected at day +21 in surviving mice (**Supplementary Figure S3**). At this time point, absolute numbers of CD4$^+$ T cells equilibrated among groups, and the sole remaining difference between groups was in the proportion of IL-17A$^+$CD4$^+$ cells. Although this proportion declined from day +14 to day +21, it remained significantly higher in Th17 coinjected mice compared with PBMC and Th0 coinjected mice at this latter time point (**Supplementary Figure S3**). Taken together, these observations suggest that in vitro Th17-polarized human cells engrafted and persisted in NSG mice.

Characterization of Human T Cells in Spleen and xGVHD Target Organs of Mice Cotransplanted with PBMC and Th17-Polarized Cells

We further assessed the composition of human T cells infiltrating spleen, BM, liver, and lungs of PBMC mice, Th17 coinjected mice, and Th0 coinjected mice at day +14 post-transplantation. We observed higher CD4$^+$/CD8$^+$ T cell ratios in BM, liver, and lungs of Th17 coinjected and Th0 coinjected mice compared with PBMC

mice (Figure 6**A**). In contrast, the spleen CD4$^+$/CD8$^+$ T cell ratio was not higher in Th17 coinjected mice compared with PBMC mice, and no significant difference was observed in absolute numbers of spleen-infiltrating CD4$^+$ T cells between Th17 coinjected and PBMC mice (Figure 6**A and B**). In the Th17 coinjected animals, a significant fraction of organ-infiltrating CD4$^+$ T cells were IL-17A$^+$ (median of 11% in BM, 12% in liver, and 10% in lungs), whereas only low levels of IL-17A$^+$ were detected in organ-derived CD4$^+$ cells from PBMC and Th0 coinjected mice (median ranging from 3% to 6% and 0 to 1%, respectively, depending on the organ) (Figure 6**C**). Consistently with these observations, we detected higher relative expression of *RORC* mRNA in target organs of Th17 coinjected mice (data not shown). Taken together, these results suggest that Th17-polarized CD4$^+$ cells migrate toward and/or proliferate in target organs of NSG mice. As observed in PB, most of IL-17A$^+$CD4$^+$ T cells acquired a double IL-17A$^+$IFNγ^+ secreting profile in peripheral tissues (median range of 72% to 85%, depending on the organ) (Figure 6**D**).

Regarding other CD4$^+$ T cell subsets, the median frequencies of IL-17A$^-$IFNγ^+ (Th1) in Th17 coinjected mice in BM, liver, and lungs were significantly lower than those observed in target organs of Th0 coinjected mice (Figure 6**E)**. The frequencies of CD4$^+$CD25$^+$FOXP3$^+$ Tregs in target organs were low in all groups, with higher proportions in PBMC mice (Figure 6**F)**. Finally, we observed higher proportions of TNFα^+CD4$^+$ cells in target organs
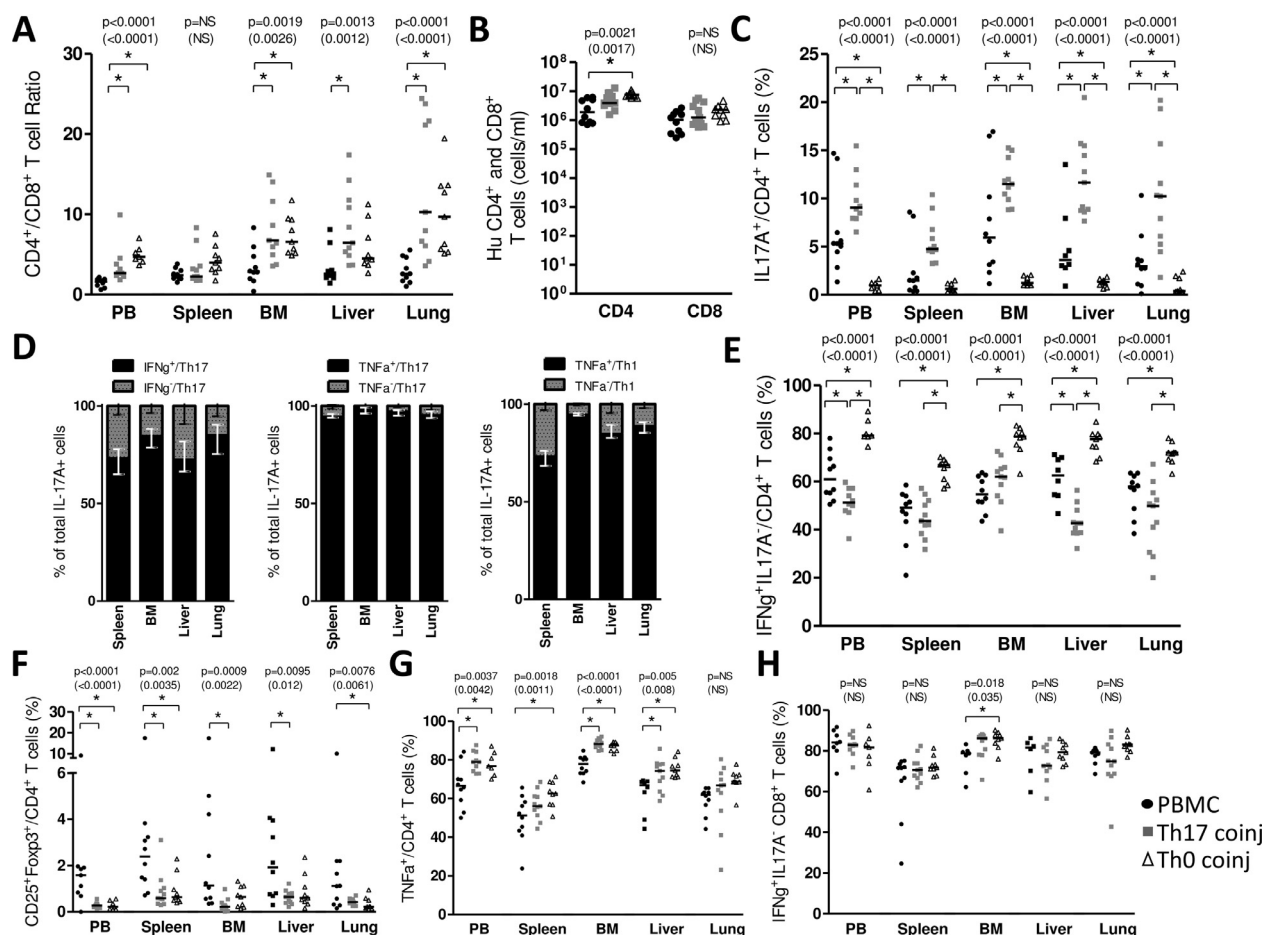
Figure 6. Human T cells in spleen and xGVHD target organs of PBMC, Th17 coinjected, and Th0 coinjected mice at day +14 after transplantation. NSG mice were irradiated (2.5 Gy total body irradiation) and then underwent transplantation with 2×10^6 PBMCs alone (PBMC mice), with 1×10^6 PBMCs combined with 1×10^6 Th17-polarized cells (Th17 coinjected mice), or with 1×10^6 nonpolarized Th0 cells (Th0 coinjected mice) from the same donor. At day +14, mice were sacrificed and PB, spleen, BM, liver, and lungs were harvested for flow cytometry analysis. (A to D) CD4$^+$/CD8$^+$ human T cell ratio (A), absolute CD4$^+$ and CD8$^+$ T cell counts in spleen (B), frequencies of IL-17A$^+$ cells among CD4$^+$ T cells (C), and frequencies of IFNγ- and TNFα-expressing cells (D) for Th17 coinjected mice. Data are median with interquartile range. (E to H) Other CD4$^+$ and CD8$^+$ T cell subsets. Data are from a single experiment with 1 donor. Global *P* values (1-way ANOVA) are shown, along with 2-by-2 group comparisons with the Scheffe post-hoc procedure (*$P < .05$). *P* values in parentheses refer to a multivariate Cox model adjusted for mouse sex and weight. Prior logarithmic transformation was applied for the CD4/CD8 T cell ratio in all organs; absolute number of CD8$^+$ T cells in spleen; percentage of IL-17A$^+$CD4$^+$ cells in spleen, liver, and lungs; and percentage of Tregs in all organs. Black circles denote PBMC mice, gray squares, Th17 coinjected mice; and white triangles, Th0 coinjected mice.

of Th17 coinjected and Th0 coinjected mice compared with PBMC mice, although the difference was not significant for lungs of Th17 coinjected mice (Figure 6**G**). TNFα was expressed by IL-17A$^+$ (Th17) and IL-17A$^-$IFNγ$^+$ (Th1) cells in high proportions (Figure 6**D**). Regarding CD8 populations, no difference was observed between Th17 coinjected mice and the other 2 groups. Most of CD8$^+$ T cells in spleen and target organs were IL-17A$^-$IFNγ$^+$ CD8$^+$ T cells (Tc1) (Figure 6**H**), and only very low (<1%) proportions of IL-17A$^+$CD8$^+$ T cells (Tc17) were detected in all groups (data not shown).

We next performed CD4$^+$IL-17A$^+$ immunohistochemical staining on liver, lung, and skin specimens harvested from mice sacrificed at day +21 after transplantation (see **Supplementary Figure S4**). In all groups of mice, we found a mild infiltration of CD4$^+$IL-17A$^+$ double-positive cells in lungs and skin (dermis) of mice, but almost a total absence of CD4$^+$IL-17A$^+$ cells in liver. We also observed a trend for a higher number of infiltrating CD4$^+$IL-17A$^+$ cells in lungs of Th17 coinjected mice compared with PBMC and Th0 coinjected mice, although the difference did not reach statistical significance. No difference in total CD4$^+$ and CD8$^+$ cell infiltration was observed between groups (data not shown).

Impact of PBMCs Cotransplanted with Th17-Polarized versus Th1-Polarized Cells on xGVHD

We next investigated the impact on xGVHD of PBMCs (1×10^6 per mouse) cotransfer with Th17-polarized cells (1×10^6 per mouse) compared with cotransfer with Th1-polarized cells (1×10^6/ mouse, Th1 coinjected group). Characteristics of in vitro polarized Th1 cells are presented in Figure 7**A**. Th17 coinjection was associated with aggravated signs of xGVHD and with lower survival compared with Th1 coinjection (*P* = .07, univariate analysis; *P* = .011, multivariate analysis) (Figure 7**B**).

Transplantation of Th17-Polarized Cells Alone (Not Combined with PBMCs)

To evaluate whether Th17-polarized cells could induce lethal xGVHD by themselves, we compared mice transplanted with Th17-polarized cells alone (2×10^6 per mouse) and mice transplanted with Th0-nonpolarized cells (2×10^6 per mouse) or Th1-polarized cells (2×10^6 per mouse) as well as a control group of PBMC mice (2×10^6 per mouse). Although they engrafted, Th17-polarized cells generated only mild xGVHD by themselves (as did Th0 and Th1 cells) (**Supplementary Figure S5**). In fact, although all PBMC mice died within 50 days
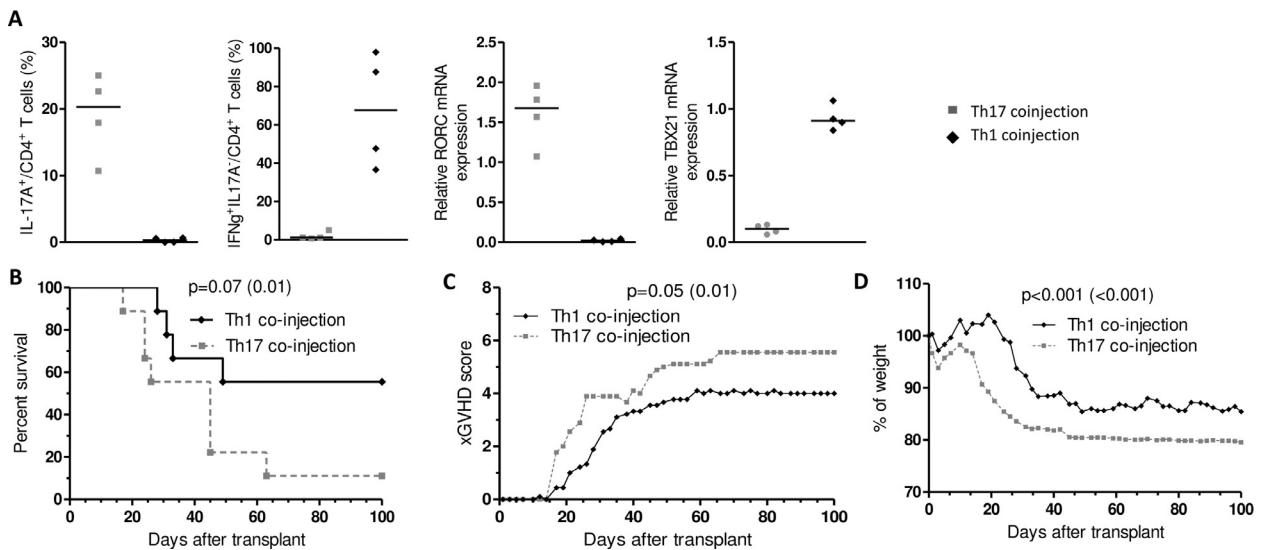
Figure 7. Impact of PBMC cotransplantation with Th17-polarized versus Th1-polarized cells on xGVHD. NSG mice were irradiated (2.5 Gy total body irradiation) and then underwent transplantation with 1×10^6 PBMCs combined with 1×10^6 Th17-polarized cells (Th17 coinjected mice) or with 1×10^6 nonpolarized Th0 cells (Th0 coinjected mice) from the same donor. (A) Frequencies of IL-17A$^+$ and IL17A$^-$IFNγ^+ cells among CD4$^+$ cells (flow cytometry) and relative mRNA expression of *RORC* and *TBX21* normalized to *TBP* (RT-qPCR). (B) Survival curves. (C) xGVHD scores. (D) Weight loss. B, C, and D show combined data from 2 replicate experiments with 2 different donors, with 7 Th17 coinjected mice and 7 Th1 coinjected mice. For xGVHD score and % of weight loss, data are shown as mean. *P* values in parentheses refer to a multivariate Cox model adjusted for PBMC donor and mouse sex and weight. Gray squares denote Th17 coinjected mice; black diamonds, Th1 coinjected mice.

after transplantation, most of Th0- and Th17-transplanted mice and all Th1-transplanted mice survived for >100 days.

Impact of PBMC Cotransplantation with Th17-Polarized Cells on GVT Effects

We evaluated the growth of THP-1-luc tumors in NSG mice that underwent transplantation with 1×10^6 freshly isolated PBMCs (PBMC group) and with 5×10^5 freshly isolated PBMCs added with 5×10^5 Th17-polarized cells (Th17 coinjection group), Th1-polarized cells (Th1 coinjection group), or nonpolarized CD4$^+$ T cells (Th0 coinjection group) (Figure 8A). As a positive control, another group of mice received s.c. injections of THP-1-luc cells without undergoing previous irradiation or transplantation with human immune cells (THP-1 control group). Compared with THP-1 control mice, decreased tumor burdens were observed in mice transplanted with human immune cells at day +21 (bioluminescent imaging, although not significant for PBMC and Th17 mice) and day +35 (tumor dissection and weighing) after THP-1-luc injection, suggesting possible GVT effects (Figure 8B and C). By analyzing the transplanted groups, we observed trends for lower bioluminescence and lower tumor weights at day +35 in Th1 coinjected mice compared with PBMC mice (Figure 8B and C). These observations may suggest that GVT effects could have been reinforced by the addition of Th1-polarized cells. In contrast, no difference was observed between Th17 coinjected and PBMC mice at both time points, suggesting that PBMC enrichment with Th17-polarized cells did not increase GVT effects.

No mouse died because of xGVHD during the experiment. Some cutaneous lesions (alopecia and skin inflammation) were observed. These skin lesions developed in several mice of each transplanted group but were more extensive in Th17 coinjected mice (**Supplementary Figure S6**).

DISCUSSION

The role of Th17 cells in the NSG xGVHD model has not yet been fully explored. In this study, we investigated the impact of PBMC cotransfer with in vitro Th17-polarized human CD4$^+$ T

cells. Compared with mice transplanted with PBMCs only or cotransplanted with PBMCs and Th0 cells, Th17 coinjected mice displayed higher frequencies and higher absolute numbers of circulating IL-17A$^+$CD4$^+$ T cells in PB, as well as higher frequencies of infiltrating IL-17A$^+$CD4$^+$ T cells in BM, liver, and lungs. Although no in vivo tracking of human lymphocytes in NSG mice was achievable, these results could provide indirect evidence that in vitro polarized Th17 cells engrafted and migrated toward target organs after transfer in recipient mice. Interestingly, the proportion of circulating IL-17A-expressing cells among CD4$^+$ T cells declined from day +14 to day +21 in Th17 coinjected mice, and only a mild CD4$^+$IL-17A$^+$ cell infiltration in organs was detected by immunohistochemistry on day +21. Although a genuine loss of the population cannot be precluded, these data are in accordance with observations reported by Gartlan et al. [11] in a mouse-to-mouse Th17 "fate-mapping" reporter model. These authors demonstrated that the expression of IL-17A protein in Th17 cells declined during the progression of GVHD, suggesting that IL-17A probably is not the most reliable marker for tracking Th17 cells in vivo. On the other hand, although most Th17-polarized cells did not produce IFNγ in vitro, we observed that the majority of IL-17A$^+$CD4$^+$ T cells coexpressed IFNγ in vivo in recipient mice, and that the proportion of IL-17A$^+$IFNγ^+-double-expressing cells increased from day +14 to day +21. These data are consistent with the concept that Th17 cells have a plastic expression profile and can convert to a "Th1-like" phenotype in vivo in the presence of the antigen and several specific cytokines, such as IFNγ itself, IL-12, and IL-23 [5,11,43,47,48]. Moreover, IFNγ expression by Th17 cells is currently recognized as a hallmark of enhanced pathogenicity and inflammatory properties [49,50]. Thus, our results suggest that in addition to their robust engraftment, in vitro polarized Th17 cells were able to acquire a pathogenic profile in recipient mice.

We further observed that, compared with mice injected with PBMCs only, mice coinjected with PBMCs and Th17-polarized cells experienced worse xGVHD and poorer survival. In contrast, no significant differences in xGVHD
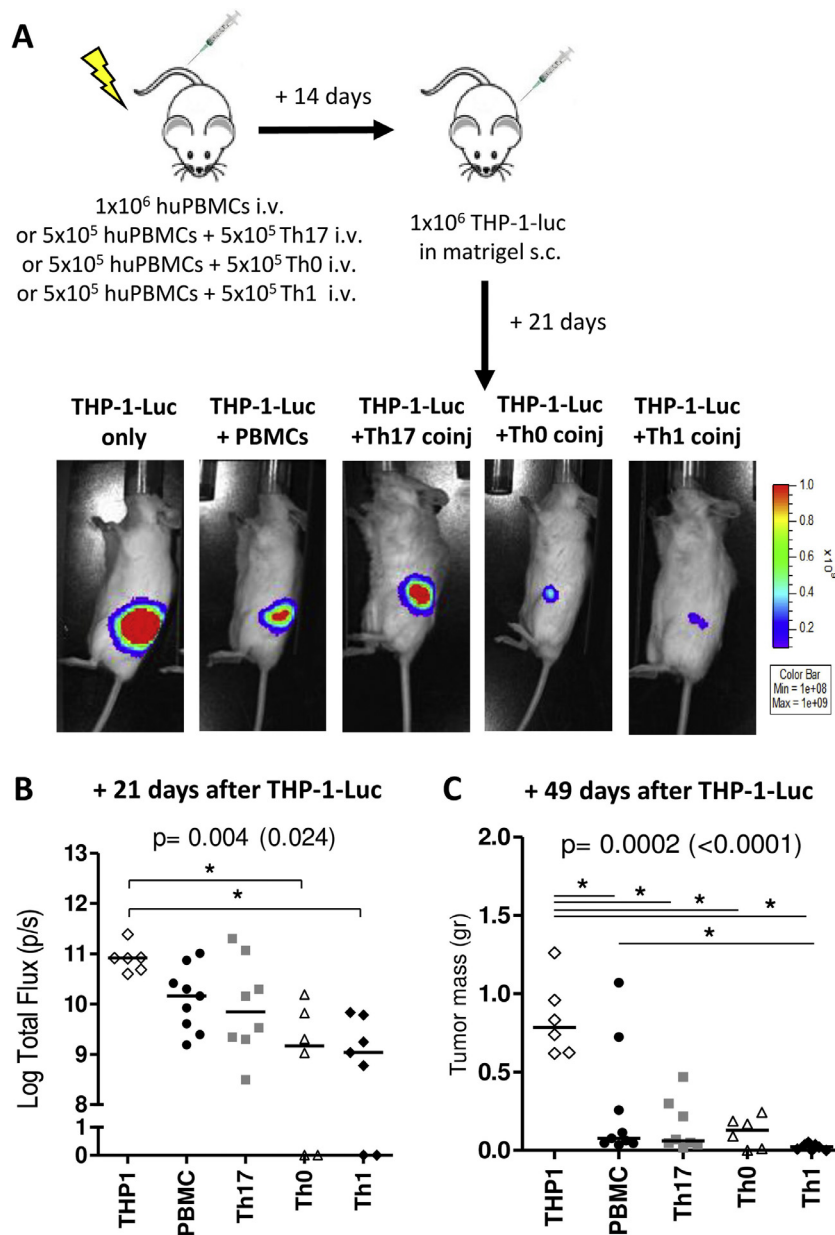
Figure 8. Impact of PBMC cotransplantation with Th17-polarized cells on GVT effects. NSG mice were irradiated (2.5 Gy total body irradiation) and then underwent transplantation with 1×10^6 PBMCs alone (PBMC mice), with 5×10^5 PBMCs combined with 5×10^5 Th17-polarized cells (Th17 coinjected mice), with 5×10^5 nonpo-larized CD4$^+$ T cells (Th0 coinjected mice), or with 5×10^5 Th1-polarized cells (Th1 coinjected mice) from the same donor. At 14 days after transplantation, mice were given an s.c. injection (in the left flank) of 1×10^6 THP-1-luc cells suspended in Matrigel solution. As a positive control, another group of mice also received an s.c. injection of THP-1-luc cells, without previous irradiation or transplantation with human immune cells (THP-1 control group). Tumor growth was evaluated by mea-suring bioluminescence at day +21 after THP-1-luc injection, and tumors were dissected and weighted at day +49 after THP-1-luc injection (planned sacrifice). (A) Images of 1 representative mouse from each group are shown, with the y-axis indicating photon flux (photons/second) measured from the mouse tumor left side. (B) Tumor bioluminescence at day +35 after injection of PBMCs with and without Th17, Th1, or Th0 coinjection. (C) Tumor weight at day +60 after injection of PBMCs with and without Th17, Th1, or Th0 coinjection. Data are from 2 independent experiments with 2 donors, 6 THP-1 mice, 9 PBMC mice, 8 Th17 coinjected mice, 6 Th0 coinjected mice, and 7 Th1 coinjected mice. Global P values (1-way ANOVA) are shown, along with 2-by-2 group comparisons with the Scheffe post-hoc procedure (*$P < .05$). P values in parentheses refer to a multivariate Cox model adjusted for PBMC donor. Black circles denote PBMC mice; gray squares, Th17 coinjected mice; white triangles, Th0 coinjected mice; black diamonds, Th1 coinjected mice.

score and survival were noted between PBMC mice and Th0 coinjected mice, suggesting that xGVHD exacerbation in mice cotransplanted with in vitro Th17-polarized cells was not simply linked to the transplantation of a greater number of CD4$^+$ T cells or to T cell preactivation during the culture process. These observations are in line with those reported in several mouse-to-mouse experiments. Using different murine models of allogeneic aGVHD, Iclozan et al. [8] and

Carlson et al. [7] demonstrated that cotransfer of T cell-depleted BM cells with in vitro differentiated mouse Th17 cells exacerbated aGVHD to a greater degree than cotransfer with purified nonactivated CD4$^+$ CD25$^-$ T cells [7] or Th0 cells [8]. Interestingly, in our experiment, in vitro generated Th0 cells contained a significant proportion of IFNγ^+CD4$^+$ cells, and most CD4$^+$ T cells in PB and peripheral organs in Th0 coinjected mice were IFNγ^+CD4$^+$ (Th1) cells.

We further examined the impact of PBMCs cotransfer with in vitro Th1-polarized cells compared with cotransfer with Th17-polarized cells. We observed lower xGVHD severity and lethality in Th1 coinjected mice compared with Th17 coinjected mice. Consistent with our observations, Iclozan et al. [8] also reported that murine Th17-polarized cells generated significantly more inflammation and damage in recipient target organs than Th1-polarized cells. Taken together, these data indicate that Th17 have a greater ability to exacerbate xGVHD than Th0 or Th1 cells in cooperation with PBMCs.

On the other hand, transplantation of Th17-polarized cells alone (not combined with PBMCs) revealed that Th17 cells did not generate lethal xGVHD by themselves, nor did Th0 and Th1 cells. This finding is in accordance with previous reports in NSG mice showing that purified CD4$^+$ T cells only mediated delayed and mild xGVHD [23,30,33,35,51]. Thus, although Th17 cells were not sufficient to individually induce lethal xGVHD, our experiments using Th17 cotransfer with PBMCs demonstrated that these cells nevertheless could exacerbate the disease.

Regarding the clinical phenotype of xGVHD mice, we noticed that some mice surviving beyond 40 days after transplantation developed cutaneous lesions (alopecia), which seemed to be more frequent and more extensive in the Th17 coinjected mice. Histopathological analyses revealed epidermal hyperplasia, epidermal and follicular dyskeratosis, basal cell layer vacuolization and dermal fibrosis. These findings are in line with several other experimental models reporting substantial IL-17A-dependent pathological cutaneous lesions [7,23]. Reports from experiments in mouse-to-mouse models of GVHD have also suggested that the lung may be highly sensitive to Th17-mediated inflammation, and that in vitro polarized murine Th17 cells are able to produce more severe lung pathological lesions than Th0 or Th1 cells [7,8]. Using our humanized xGVHD model, we similarly observed a trend for aggravated histopathological xGVHD lesions compared with PBMC and Th0 coinjected mice. However, considering the small sample size in our experiment, this remains to be confirmed in further studies.

Our present results do not reveal the mechanisms by which Th17 coinjection exacerbate xGVHD severity and lethality. Among the various hypotheses that have been advanced, previous observations from murine T cell transfer experiments have suggested a superior ability of Th17 cells to expand and infiltrate target organs compared with other Th subsets, such as Th1 cells. [8] In line with this, our CFSE experiments revealed an accelerated cell division rate in PB and target organs for human Th17-polarized cells compared with fresh CD4$^+$ T cells, Th0 cells, and Th1 cells early (day +3) after their transfer in NSG mice. However, we did not observe higher chimerism in PB at days +14 and +21 in Th17 coinjected mice. Data from antitumor and antiviral immunity experiments have also revealed that Th17 cells could have a unique ability to promote CD8$^+$ T cell priming and cytotoxicity in target tissues through both direct [52-54] and indirect (via the recruitment of dendritic cells) [52,55] mechanisms.

Whether Th17 cells can in fact enhance CD8$^+$ T cell cytotoxicity during xGVHD in our model remains to be explored in further studies.

Th17 cells are known to secrete an array of inflammatory effector cytokines that are not typically produced by Th1 cells, among which IL-17A is the most well known. We detected increased IL-17A serum titers as well as increased frequencies of IL-17A-expressing CD4$^+$ T cells in target organs in Th17

coinjected mice at day +14 after transplantation. Several previous studies have reported that disruption of IL-17A signaling (either genetically or via neutralizing antibodies) can markedly decrease skin and lung GVHD pathology [7,23,56]. IL-17 has been shown to be capable of causing direct [57] and indirect tissue damage, the latter via the induction of additional cytokines and chemokines, which in turn mobilize a variety of inflammatory leukocytes (ie, neutrophils, dendritic cells, macrophages, and other lymphocytes, such as CD8$^+$ T cells) in target tissues [23,56,58-60]. Indeed, in a mouse-to-mouse allogeneic model, Hill et al. [56] found that the major effect of IL-17A in Th17-mediated aGVHD skin lesions appeared to be as a chemoattractant for macrophages and neutrophils. Recently, Ito et al. [23] observed similar conclusions in their humanized model of CD4$^+$ T cell-mediated cutaneous xGVHD in NOG mice. They reported that inhibition of human IL-17A with secukinumab (an anti-huIL-17A monoclonal antibody) reduced neutrophil infiltration into the skin and prevented Th17-mediated skin inflammation. Taken together, these findings support a potential role of IL-17A in Th17-mediated skin and lung GVHD pathology. One specificity of the xGVHD NSG model is the gut-sparing effect [27]. In contrast, the intestine is a major target for aGVHD in humans. IL-17A has been reported to play complex roles in gut immunity, with both proinflammatory and protective effects [61]. Preclinical and clinical studies in psoriasis and inflammatory bowel disorders have revealed risks of induction or exacerbation of colitis, as well as susceptibility to infections, when using IL-17A-neutralizing approaches [20-22]. Thus, caution is warranted when considering IL-17A blockade for treating patients with aGVHD.

Other cytokines linked to Th17 functions, such as IL-17F, IL-21, IL-22, and GM-CSF [10], also might have contributed to Th17-mediated xGVHD, but these were not explored in this study.

Although Th17 cooperated with PBMCs in xGVHD reactions, Th17 cotransfer with PBMCs did not reinforce GVT effects against human THP-1 cells. The possibility that CD4$^+$ T cells have a limited role in GVT reactions compared with CD8$^+$ T cells cannot be excluded [62,63]. Moreover, Th17 cells have been reported to alternatively exert either protumor or antitumor effects, partly in line with their highly plastic developmental program, which gives them the ability to transdifferentiate toward functional distinct phenotypes, including Th17/Th1-like cells as well as suppressive IL-10$^+$ FOXP3$^+$ Th17 cells [64-68]. The context may be important, and there is a possibility that the complex tumor microenvironment can govern Th17 cell fate. However, our results must be interpreted with caution, considering the complex and artificial nature of our model with s.c. injection of human THP-1 cells.

To the best of our knowledge, only a few experimental xGVHD models allow the exploration of human Th17 cell behavior in vivo. In addition to the model of Th17-mediated cutaneous xGVHD recently developed by Ito et al. [23], which does not allow for investigation of the impact of Th17 on CD8$^+$ T cells, we believe that the model we present here may offer a relevant preclinical platform for exploring pathological pathways mediated by human Th17 in GVHD and GVT immunobiology. However, we must concede some limitations of our model that suggest the need for a caution when interpreting our results. The first of these was the difficulty in generating highly enriched and purified populations of IL-17A-expressing cells from human naive CD4$^+$ T cells in vitro. In accordance with our results, Kleinewietfeld et al. [42] also reported a median IL-17A$^+$CD4$^+$ T cell yield of 5% to 35% after in vitro differentiation from human naive T cells. These

results are in opposition to previous reports from mouse experiment that showed stable generation of highly purified Th17 from naive mouse CD4$^+$ T cells [7,43-45], supporting the concept of differences between human and mouse Th17 immunology. Nevertheless, although they contained only a limited fraction of IL-17A$^+$ expressing cells, Th17-polarized cells had a major impact on xGVHD in our study. On the other hand, the fact that the in vitro generated population of human Th17-polarized CD4$^+$ T cells was heterogeneous in nature and not a pure subset of Th17 lymphocytes may raise concerns regarding their actual implications in xGVHD exacerbation. We believe that experiments with the comparative group of Th0 coinjected mice showing that xGVHD was not exacerbated by the cotransfer of Th0 cells and that the main differences between Th0 coinjected and Th17 coinjected mice concerned IL-17A$^+$CD4$^+$ frequencies may raise some arguments regarding the fact that Th17 cells were likely the effector cells responsible for aggravated xGVHD.

Finally, along with the impact of Th17 coinjection, results from the first set of our experiments (PBMC versus Th17 coinjection, 4 different donors) also suggested significant interdonor variability in xGVHD severity and lethality. This finding is in accordance with previous reports from our group [34] and others [29]. Compared with mouse-to-mouse allogeneic models of aGVHD characterized by fixed genetic and immunologic disparities between donors and recipients (within a determined model), this xGVHD model uses human PBMC donors with high genetic diversity. Moreover, whereas mice are bred and housed in pathogen-free conditions, human donors are exposed to pathogens than can variously influence their immunity (eg, the relationship between CMV infection and GVHD [69]). However, specific predictors of donor xenoreactivity in this model remain to be determined.

In conclusion, our current observations point out the potential functional implication of human Th17 cells in xGVHD immunopathology and support exploring Th17 targeted strategies for intervention to reduce aGVHD.

ACKNOWLEDGMENTS

SUPPLEMENTARY DATA

Supplementary data related to this article can be found online at doi:10.1016/j.bbmt.2018.10.007.

REFERENCES

1. Servais S, Beguin Y, Delens L, et al. Novel approaches for preventing acute graft-versus-host disease after allogeneic hematopoietic stem cell transplantation. *Expert Opin Investig Drugs.* 2016;25:957−972.
2. Zeiser R, Socié G, Blazar BR. Pathogenesis of acute graft-versus-host disease: from intestinal microbiota alterations to donor T cell activation. *Br J Haematol.* 2016;175:191−207.
3. Zeiser R, Blazar BR. Acute graft-versus-host disease: biologic process, prevention, and therapy. *N Engl J Med.* 2017;377:2167−2179.
4. Aversa F, Tabilio A, Velardi A, et al. Treatment of high-risk acute leukemia with T-cell-depleted stem cells from related donors with one fully mismatched HLA haplotype. *N Engl J Med.* 1998;339:1186−1193.
5. Muranski P, Restifo NP. Essentials of Th17 cell commitment and plasticity. *Blood.* 2013;121:2402−2414.
6. Lu SX, Alpdogan O, Lin J, et al. STAT-3 and ERK 1/2 phosphorylation are critical for T-cell alloactivation and graft-versus-host disease. *Blood.* 2008;112:5254−5258.
7. Carlson MJ, West ML, Coghill JM, Panoskaltsis-Mortari A, Blazar BR, Serody JS. In vitro-differentiated Th17 cells mediate lethal acute graft-versus-host disease with severe cutaneous and pulmonary pathologic manifestations. *Blood.* 2009;113:1365−1374.
8. Iclozan C, Yu Y, Liu C, et al. T helper17 cells are sufficient but not necessary to induce acute graft-versus-host disease. *Biol Blood Marrow Transplant.* 2010;16:170−178.
9. Kappel LW, Goldberg GL, King CG, et al. IL-17 contributes to CD4-mediated graft-versus-host disease. *Blood.* 2009;113:945−952.
10. Malard F, Gaugler B, Lamarthee B, Mohty M. Translational opportunities for targeting the Th17 axis in acute graft-vs.-host disease. *Mucosal Immunol.* 2016;9:299−308.
11. Gartlan KH, Varelias A, Koyama M, et al. Th17 plasticity and transition toward a pathogenic cytokine signature are regulated by cyclosporine after allogeneic SCT. *Blood Adv.* 2017;1:341−351.
12. Liu Y, Cai Y, Dai L, et al. The expression of Th17-associated cytokines in human acute graft-versus-host disease. *Biol Blood Marrow Transplant.* 2013;19:1421−1429.
13. Bossard C, Malard F, Arbez J, et al. Plasmacytoid dendritic cells and Th17 immune response contribution in gastrointestinal acute graft-versus-host disease. *Leukemia.* 2012;26:1471−1474.
14. Betts BC, Sagatys EM, Veerapathran A, et al. CD4$^+$ T cell STAT3 phosphorylation precedes acute GVHD, and subsequent Th17 tissue invasion correlates with GVHD severity and therapeutic response. *J Leukoc Biol.* 2015;97:807−819.
15. Elmaagacli AH, Koldehoff M, Landt O, Beelen DW. Relation of an interleukin-23 receptor gene polymorphism to graft-versus-host disease after hematopoietic-cell transplantation. *Bone Marrow Transplant.* 2008;41: 821−826.
16. Broady R, Yu J, Chow V, et al. Cutaneous GVHD is associated with the expansion of tissue-localized Th1 and not Th17 cells. *Blood.* 2010;116: 5748−5751.
17. Ratajczak P, Janin A, Peffault de Latour R, et al. Th17/Treg ratio in human graft-versus-host disease. *Blood.* 2010;116:1165−1171.
18. Nguyen Y, Al-Lehibi A, Gorbe E, et al. Insufficient evidence for association of NOD2/CARD15 or other inflammatory bowel disease-associated markers on GVHD incidence or other adverse outcomes in T-replete, unrelated donor transplantation. *Blood.* 2010;115:3625−3631.
19. Ernst PB, Carvunis AR. Of mice, men and immunity: a case for evolutionary systems biology. *Nat Immunol.* 2018;19:421−425.
20. Targan SR, Feagan B, Vermeire S, et al. A randomized, double-blind, placebo-controlled phase 2 study of brodalumab in patients with moderate-to-severe Crohn's disease. *Am J Gastroenterol.* 2016;111:1599−1607.
21. Hueber W, Sands BE, Lewitzky S, et al. Secukinumab, a human anti-IL-17A monoclonal antibody, for moderate to severe Crohn's disease: unexpected results of a randomised, double-blind placebo-controlled trial. *Gut.* 2012;61:1693−1700.
22. Hohenberger M, Cardwell LA, Oussedik E, Feldman SR. Interleukin-17 inhibition: role in psoriasis and inflammatory bowel disease. *J Dermatolog Treat.* 2018;29:13−18.
23. Ito R, Katano I, Kawai K, et al. A novel xenogeneic graft-versus-host disease model for investigating the pathological role of human CD4$^+$ or CD8$^+$ T cells using immunodeficient NOG mice. *Am J Transplant.* 2017;17: 1216−1228.
24. Ito R, Katano I, Kawai K, et al. Highly sensitive model for xenogenic GVHD using severe immunodeficient NOG mice. *Transplantation.* 2009;87: 1654−1658.
25. Hannon M, Lechanteur C, Lucas S, et al. Infusion of clinical-grade enriched regulatory T cells delays experimental xenogeneic graft-versus-host disease. *Transfusion.* 2014;54:353−363.
26. Ehx G, Fransolet G, de Leval L, et al. Azacytidine prevents experimental xenogeneic graft-versus-host disease without abrogating graft-versus-leukemia effects. *Oncoimmunology.* 2017;6 e1314425.
27. Burlion A, Brunel S, Petit NY, Olive D, Marodon G. Targeting the human T-cell inducible COStimulator molecule with a monoclonal antibody prevents graft-vs-host disease and preserves graft vs leukemia in a xenograft murine model. *Front Immunol.* 2017;8:756.

28. Cuende J, Liénart S, Dedobbeleer O, et al. Monoclonal antibodies against GARP/TGF-ß1 complexes inhibit the immunosuppressive activity of human regulatory T cells in vivo. *Sci Transl Med*. 2015;7:284ra56.

29. Kawasaki Y, Sato K, Hayakawa H, et al. Comprehensive analysis of the activation and proliferation kinetics and effector functions of human lymphocytes, and antigen presentation capacity of antigen-presenting cells in xenogeneic graft-versus-host disease. *Biol Blood Marrow Transplant*. 2018;24:1563–1574.

30. King MA, Covassin L, Brehm MA, et al. Human peripheral blood leucocyte non-obese diabetic-severe combined immunodeficiency interleukin-2 receptor gamma chain gene mouse model of xenogeneic graft-versus-host-like disease and the role of host major histocompatibility complex. *Clin Exp Immunol*. 2009;157:104–118.

31. van Rijn RS, Simonetti ER, Hagenbeek A, et al. A new xenograft model for graft-versus-host disease by intravenous transfer of human peripheral blood mononuclear cells in RAG2$^{−/−}$gammac$^{−/−}$double-mutant mice. *Blood*. 2003;102:2522–2531.

32. Betts BC, Veerapathran A, Pidala J, et al. Targeting Aurora kinase A and JAK2 prevents GVHD while maintaining Treg and antitumor CTL function. *Sci Transl Med*. 2017;9. eaai8269.

33. Covassin L, Laning J, Abdi R, et al. Human peripheral blood CD4 T cell-engrafted non-obese diabetic-scid IL2rγ(null) H2-Ab1 (tm1Gru) Tg (human leucocyte antigen D-related 4) mice: a mouse model of human allogeneic graft-versus-host disease. *Clin Exp Immunol*. 2011;166:269–280.

34. Ehx G, Somja J, Warnatz HJ, et al. Xenogeneic graft-versus-host disease in humanized NSG and NSG-HLA-A2/HHD mice. *Front Immunol*. 2018;9:1943.

35. Sùndergaard H, Kvist PH, Haase C. Human T cells depend on functional calcineurin, tumour necrosis factor-α and CD80/CD86 for expansion and activation in mice. *Clin Exp Immunol*. 2013;172:300–310.

36. Hippen KL, Bucher C, Schirm DK, et al. Blocking IL-21 signaling ameliorates xenogeneic GVHD induced by human lymphocytes. *Blood*. 2012;119:619–628.

37. Bruck F, Belle L, Lechanteur C, et al. Impact of bone marrow-derived mesenchymal stromal cells on experimental xenogeneic graft-versus-host disease. *Cytotherapy*. 2013;15:267–279.

38. Gregoire-Gauthier J, Durrieu L, Duval A, et al. Use of immunoglobulins in the prevention of GvHD in a xenogeneic NOD/SCID/γc- mouse model. *Bone Marrow Transplant*. 2012;47:439–450.

39. Coulie PG, Stevens M, Van Snick J. High- and low-affinity receptors for murine interleukin 6: distinct distribution on B and T cells. *Eur J Immunol*. 1989;19:2107–2114.

40. Hammacher A, Ward LD, Weinstock J, Treutlein H, Yasukawa K, Simpson RJ. Structure-function analysis of human IL-6: identification of two distinct regions that are important for receptor binding. *Protein Sci*. 1994;3:2280–2293.

41. Hatano R, Ohnuma K, Yamamoto J, Dang NH, Yamada T, Morimoto C. Prevention of acute graft-versus-host disease by humanized anti-CD26 monoclonal antibody. *Br J Haematol*. 2013;162:263–277.

42. Kleinewietfeld M, Manzel A, Titze J, et al. Sodium chloride drives autoimmune disease by the induction of pathogenic TH17 cells. *Nature*. 2013;496:518–522.

43. Ghoreschi K, Laurence A, Yang XP, et al. Generation of pathogenic T(H)17 cells in the absence of TGF-ß signalling. *Nature*. 2010;467:967–971.

44. Lee Y, Awasthi A, Yosef N, et al. Induction and molecular signature of pathogenic TH17 cells. *Nat Immunol*. 2012;13:991–999.

45. McGeachy MJ, Bak-Jensen KS, Chen Y, et al. TGF-beta and IL-6 drive the production of IL-17 and IL-10 by T cells and restrain T(H)-17 cell-mediated pathology. *Nat Immunol*. 2007;8:1390–1397.

46. Acosta-Rodriguez EV, Rivino L, Geginat J, et al. Surface phenotype and antigenic specificity of human interleukin 17-producing T helper memory cells. *Nat Immunol*. 2007;8:639–646.

47. Lee YK, Turner H, Maynard CL, et al. Late developmental plasticity in the T helper 17 lineage. *Immunity*. 2009;30:92–107.

48. Mukasa R, Balasubramani A, Lee YK, et al. Epigenetic instability of cytokine and transcription factor gene loci underlies plasticity of the T helper 17 cell lineage. *Immunity*. 2010;32:616–627.

49. Wang Y, Godec J, Ben-Aissa K, et al. The transcription factors T-bet and Runx are required for the ontogeny of pathogenic interferon-γ-producing T helper 17 cells. *Immunity*. 2014;40:355–366.

50. El-Behi M, Ciric B, Dai H, et al. The encephalitogenicity of T(H)17 cells is dependent on IL-1- and IL-23-induced production of the cytokine GM-CSF. *Nat Immunol*. 2011;12:568–575.

51. King M, Pearson T, Shultz LD, et al. A new Hu-PBL model for the study of human islet alloreactivity based on NOD-scid mice bearing a targeted mutation in the IL-2 receptor gamma chain gene. *Clin Immunol*. 2008;126:303–314.

52. Ankathatti Munegowda M, Deng Y, Mulligan SJ, Xiang J. Th17 and Th17-stimulated CD8$^+$ T cells play a distinct role in Th17-induced preventive and therapeutic antitumor immunity. *Cancer Immunol Immunother*. 2011;60:1473–1484.

53. Hemmi M, Tachibana M, Fujimoto N, et al. T helper 17 promotes induction of antigen-specific gut-mucosal cytotoxic T lymphocytes following adenovirus vector vaccination. *Front Immunol*. 2017;8:1456.

54. Acharya D, Wang P, Paul AM, et al. Interleukin-17A promotes CD8+ T cell cytotoxicity to facilitate West Nile virus clearance. *J Virol*. 2016;91. e01529-16.

55. Martin B, Hirota K, Cua DJ, Stockinger B, Veldhoen M. Interleukin-17-producing gammadelta T cells selectively expand in response to pathogen products and environmental signals. *Immunity*. 2009;31:321–330.

56. Hill GR, Olver SD, Kuns RD, et al. Stem cell mobilization with G-CSF induces type 17 differentiation and promotes scleroderma. *Blood*. 2010;116:819–828.

57. Qian Y, Liu C, Hartupee J, et al. The adaptor Act1 is required for interleukin 17-dependent signaling associated with autoimmune and inflammatory disease. *Nat Immunol*. 2007;8:247–256.

58. Korn T, Bettelli E, Oukka M, Kuchroo VK. IL-17 and Th17 cells. *Annu Rev Immunol*. 2009;27:485–517.

59. Liu Y, Mei J, Gonzales L, et al. IL-17A and TNF-α exert synergistic effects on expression of CXCL5 by alveolar type II cells in vivo and in vitro. *J Immunol*. 2011;186:3197–3205.

60. Bulek K, Liu C, Swaidani S, et al. The inducible kinase IKKi is required for IL-17-dependent signaling associated with neutrophilia and pulmonary inflammation. *Nat Immunol*. 2011;12:844–852.

61. Veldhoen M. Interleukin 17 is a chief orchestrator of immunity. *Nat Immunol*. 2017;18:612–621.

62. Ueha S, Yokochi S, Ishiwata Y, et al. Combination of anti-CD4 antibody treatment and donor lymphocyte infusion ameliorates graft-versus-host disease while preserving graft-versus-tumor effects in murine allogeneic hematopoietic stem cell transplantation. *Cancer Sci*. 2017;108:1967–1973.

63. Ni X, Song Q, Cassady K, et al. PD-L1 interacts with CD80 to regulate graft-versus-leukemia activity of donor CD8$^+$ T cells. *J Clin Invest*. 2017;127:1960–1977.

64. Bailey SR, Nelson MH, Himes RA, Li Z, Mehrotra S, Paulos CM. Th17 cells in cancer: the ultimate identity crisis. *Front Immunol*. 2014;5:276.

65. Downs-Canner S, Berkey S, Delgoffe GM, et al. Suppressive IL-17A$^+$Foxp3$^+$ and ex-Th17 IL-17A$^−$Foxp3$^+$ Treg cells are a source of tumour-associated Treg cells. *Nat Commun*. 2017;8:14649.

66. Gagliani N, Amezcua Vesely MC, Iseppon A, et al. Th17 cells transdifferentiate into regulatory T cells during resolution of inflammation. *Nature*. 2015;523:221–225.

67. Hirota K, Turner JE, Villa M, et al. Plasticity of Th17 cells in Peyer's patches is responsible for the induction of T cell-dependent IgA responses. *Nat Immunol*. 2013;14:372–379.

68. Voo KS, Wang YH, Santori FR, et al. Identification of IL-17-producing FOXP3$^+$ regulatory T cells in humans. *Proc Natl Acad Sci U S A*. 2009;106:4793–4798.

69. Cantoni N, Hirsch HH, Khanna N, et al. Evidence for a bidirectional relationship between cytomegalovirus replication and acute graft-versus-host disease. *Biol Blood Marrow Transplant*. 2010;16:1309–1314.